Neuro-Oncology Advances

Neuronal differentiation drives the antitumor activity of mitogen-activated protein kinase kinase (MEK) inhibition in glioblastoma

Sabbir Khan, Emmanuel Martinez-Ledesma, Jianwen Dong, Rajasekaran Mahalingam, Soon Young Park, Yuji Piao, Dimpy Koul, Veerakumar Balasubramaniyan, John F. de Groot, and W.K. Alfred Yung

Department of Neuro-Oncology, University of Texas MD Anderson Cancer Center, Houston, Texas, USA (S.K., E.M.-L., J.D., S.Y.P., Y.P., D.K., V.B., J.F.G., W.K.A.Y.); Tecnologico de Monterrey, Escuela de Medicina y Ciencias de la Salud, Monterrey, Nuevo León, Mexico (E.M.-L.); Tecnologico de Monterrey, Institute for Obesity Research, Monterrey, Nuevo León, Mexico (E.M.-L.); Department of Symptom Research, University of Texas MD Anderson Cancer Center, Houston, Texas, USA (R.M.); Department of Neurosurgery, University of California-San Francisco, San Francisco, California, USA (J.F.G.)

Corresponding Authors: W. K. Alfred Yung, MD, Department of Neuro-Oncology, University of Texas MD Anderson Cancer Center, 1515 Holcombe Blvd., Houston, TX 77030, USA (wyung@mdanderson.org); John F. de Groot, MD, Department of Neurosurgery, University of California-San Francisco, San Francisco, CA 94143, USA (John.deGroot@ucsf.edu).

Abstract

Background. Epidermal growth factor receptor (EGFR) amplification is found in nearly 40%–50% of glioblastoma cases. Several EGFR inhibitors have been tested in glioblastoma but have failed to demonstrate long-term therapeutic benefit, presumably because of acquired resistance. Targeting EGFR downstream signaling with mitogen-activated protein kinase kinase 1 and 2 (MEK1/2) inhibitors would be a more effective approach to glioblastoma treatment. We tested the therapeutic potential of MEK1/2 inhibitors in glioblastoma using 3D cultures of glioma stem-like cells (GSCs) and mouse models of glioblastoma.

Methods. Several MEK inhibitors were screened in an unbiased high-throughput platform using GSCs. Cell death was evaluated using flow cytometry and Western blotting (WB) analysis. RNA-seq, real-time quantitative polymerase chain reaction, immunofluorescence, and WB analysis were used to identify and validate neuronal differentiation.

Results. Unbiased screening of multiple MEK inhibitors in GSCs showed antiproliferative and apoptotic cell death in sensitive cell lines. An RNA-seq analysis of cells treated with trametinib, a potent MEK inhibitor, revealed upregulation of neurogenesis and neuronal differentiation genes, such as achaete-scute homolog 1 (ASCL1), delta-like 3 (DLL3), and neurogenic differentiation 4 (NeuroD4). We validated the neuronal differentiation phenotypes in vitro and in vivo using selected differentiation markers (β-III-tubulin, ASCL1, DLL3, and NeuroD4). Oral treatment with trametinib in an orthotopic GSC xenograft model significantly improved animal survival, with 25%–30% of mice being long-term survivors.

Conclusions. Our findings demonstrated that MEK1/2 inhibition promotes neuronal differentiation in glioblastoma, a potential additional mechanism of action of MEK1/2 inhibitors. Thus, MEK inhibitors could be efficacious in glioblastoma patients with activated EGFR/MAPK signaling.

Key Points

- Glioblastoma tumors exhibit heterogeneous amplification of EGFR and downstream signaling.
- MEK inhibitors screening indicated differential activity in GSCs with activated EGFR/MAPK signaling.
- Neuronal differentiation contributes to the antitumor activity of MEK inhibitors in glioblastoma.

Graphical Abstract
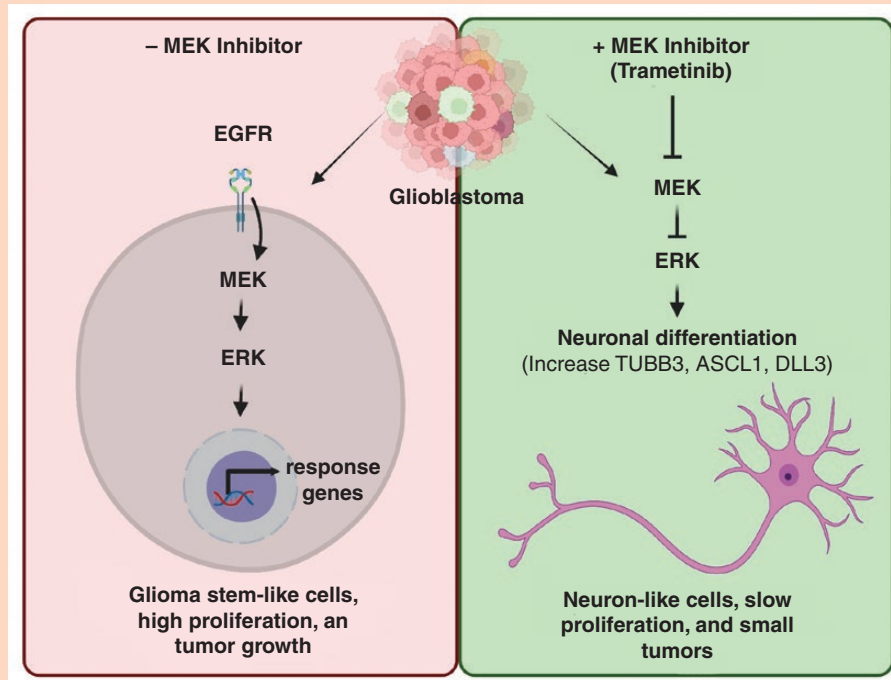
Importance of the Study

Long-term therapy with EGFR inhibitors in glioblastoma has been unsuccessful, presumably because of the activation of escape signaling pathways and acquired resistance. We found that multiple mitogen-activated protein kinase kinase 1 and 2 (MEK1/2) inhibitors show preferential antiproliferative and antitumor effects in GSCs and in mouse glioblastoma with activated EGFR/ MEK/ERK signaling. A mechanistic investigation revealed that neuronal differentiation contributes to the antitumor activity of MEK inhibitors. This study provides evidence for neuronal differentiation as a potential mechanism of action of MEK inhibitors and their application in the treatment of glioblastoma patients with activated EGFR/MAPK signaling tumors.

Glioblastoma is highly resistant to standard-of-care treatment; therefore, recurrence frequently occurs.[1] Over the past decade, despite our improved understanding of glioblastoma biology at the transcriptomic and epigenomic levels, advances in treatment have been limited. The molecular heterogeneity of glioblastoma is recapitulated in glioma stem-like cells (GSCs), which are known for their clonal heterogeneity and plasticity.[2,3] These challenging features are likely to influence disease progression and response to various treatment modalities.[4] Several studies have characterized epidermal growth factor receptor (EGFR) genomic alterations and amplification in nearly 40%–50% of glioblastoma cases.[5–8] In addition, a recent study described the role of the mitogen-activated protein kinase (MAPK) pathway in the subclassification of isocitrate dehydrogenase 1 (IDH1)-wild-type glioblastoma for diagnostic, prognostic, and therapeutic inferences.[9] EGFR plays a critical role in tumorigenesis and the proliferation and survival of glioblastoma cells via

the activation of the phosphoinositide 3-kinase-protein kinase B (PI3K/AKT), MAPK, and Janus kinase-signal transducer and activator of transcription 3 (JAK/STAT3) signaling pathways.[10,11] EGFR/MAPK initiates a downstream signaling cascade to phosphorylate the nuclear protein Jun (a transcription factor), which forms complexes with different nuclear proteins and is involved in tumor growth and cell proliferation.[12]

Several EGFR inhibitors, such as erlotinib and gefitinib, have been developed to target EGFR signaling in glioblastoma but have failed to demonstrate long-term therapeutic benefit, despite active EGFR signaling.[13] Other attempts to target EGFR or the common mutant EGFR variant III (EGFR-VIII) using monoclonal antibodies and EGFR-VIII–directed immunotherapy are currently being explored.[14] However, a major hurdle in targeting EGFR for clinical application is the widespread intra-tumoral heterogeneity of EGFR alterations and acquired resistance caused by the activation of escape signaling. Therefore, targeting EGFR downstream

signaling with MEK1/2 inhibitors might be a better therapeutic approach to the treatment of glioblastoma.

The MEK1/2/extracellular signal-regulated kinase (ERK-1/2) pathway has been implicated in several cellular aspects of glioblastoma, such as migration and invasion.[15] Furthermore, MEK1/2/ERK-1/2 signaling was found to play an important role in the maintenance of stemness and cell proliferation and differentiation.[15,16] Several MEK1/2 inhibitors have been tested clinically or are currently undergoing clinical evaluation for cancer therapy.[17] Trametinib is the first MEK1/2 inhibitor approved by the FDA as a single agent for the treatment of metastatic melanoma with BRAF V600E mutation, which was used in combination with dabrafenib to overcome drug resistance.[18] A recent clinical trial of trametinib in combination with dabrafenib showed good efficacy in patients with BRAF V600E mutation–positive recurrent or refractory high- and low-grade glioma.[19] Moreover, another MEK inhibitor, selumetinib, is approved for the treatment of neurofibromatosis type I, a genetic disorder of the nervous system that causes nerve tumors in children.[20] Thus, it is pertinent to further investigate the mechanism of MEK inhibitors to explore their full potential in cancer treatment.

We hypothesized that targeting EGFR downstream signaling with MEK1/2 inhibitors would be a more effective approach to glioblastoma treatment. In this study, we tested the therapeutic potential of MEK1/2 inhibitors in glioblastoma using 3D culture of GSCs and a mouse model of glioblastoma. Our findings demonstrated the antiproliferative and antitumor activity of MEK1/2 inhibitors is mainly by promoting neuronal differentiation thus providing a rationale for the use of these agents for effective treatment for glioblastoma patients with active EGFR/MAPK signaling.

Materials and Methods

Bioinformatics and Analyses of The Cancer Genome Atlas and Other Public Data sets

The Cancer Genome Atlas (TCGA) glioblastoma microarray and RNA-seq data sets were downloaded from the FireBrowse site of the Broad Institute.[21] We used Affymetrix U-133 microarray and RNA-seq data for gene expression. EGFR amplification was defined according to the thresholds assigned by genomic identification of significant targets in cancer (GISTIC) (–2, –1, 0, 1, and 2, where 2 is defined as focal amplification).[22] We defined copy number events according to the number of EGFR (egfr)- or centromere (cent)-stained cells. The copy number events were as follows: (a) deletion: (egfr == 0 AND cent > 0) or (egfr < cent); (b) ploidy: (egfr == cent) and (egfr < threshold); (c) broad amplification: (egfr/cent) < 2; and (d) focal amplification: ([egfr/cent] ≥ 2) or (cent == 0 and egfr > 0). The RNA-seq data set of GSCs (42 lines) was analyzed for EGFR amplification and expression profile. All the statistical analyses were performed using R unless otherwise specified. In addition, the GlioVis platform[23] was used to analyze the gene expression of various neuronal differentiation markers and survival in glioblastoma tumors using TCGA data.[24] A Kaplan–Meier survival analysis was performed with low and high expression of selected neuronal differentiation markers in glioma/glioblastoma tumors using TCGA,[24] Chinese Glioma Genome Atlas,[25] and Rembrandt[26] data sets.

Cell Lines and Reagents

GSCs were isolated from patient-derived surgical specimens at the University of Texas MD Anderson Cancer Center, as previously described,[27] and approved by the institutional review board (protocol #LAB04-0001). The GSCs were grown and maintained in suspension culture in Dulbecco's modified Eagle medium (DMEM, Corning, NY, USA), supplemented with 2% B-27 (Thermo Fisher Scientific, Waltham, MA, USA), epidermal growth factor (EGF), basic fibroblast growth factor (FGF), and antibiotics at 37°C in a 5% CO_2 atmosphere, as described previously.[28] Short tandem repeats using the Applied Biosystems AmpFlSTR identifier kit (Foster City, CA, USA) were used to authenticate cells. All the GSCs lines used in this study are isocitrate dehydrogenase wild-type (IDHwt) except GSC5-22. The EGFR amplification in GSCs lines was characterized as described in the previous study.[29] All MEK inhibitors (GDC-0623, MEK162, RO5126766 [RO5], and trametinib) were purchased from (Selleckchem, Houston, TX, USA). All cell lines tested negative for mycoplasma contamination using the MycoAlert Detection Kit (Lonza, Houston, TX, USA).

Drug Screening, Cell Viability, and IC_{50} Calculation

Cell viability or proliferation with MEK inhibitor treatment was evaluated using a luminescence-based cell viability assay (CellTiter-Glo) kit from Promega (Madison, WI, USA) according to the manufacturer's protocol. The GSCs (1–5×10^3 per well) were cultured in 384- or 96-well white plates and treated with the specific inhibitors for the indicated times. The relative cell viability was calculated using control (untreated) cells for each plate. The IC_{50} was calculated using GraphPad Prism software (GraphPad Software, Inc.) as a function of the drug concentration required to inhibit cell proliferation by 50% as compared with untreated cells.

Fluorescence In Situ Hybridization

A fluorescence in situ hybridization (FISH) assay was performed on human and mouse glioblastoma tumor slides using an EGFR-FISH probe from Empire Genomics, as per the manufacturer's instructions, as described previously.[29] In brief, the probe was applied to the slides, covered with a glass coverslip, and sealed with rubber cement. The slides were denatured at 70°C using the ThermoBrite system (Abbott Laboratories, Chicago, IL, USA) and incubated at 37°C overnight. The slides were washed with sodium citrate buffer at 45°C for 1–2 min, rinsed in PBS containing 0.05% v/v Tween-20, and counterstained with DAPI. The slides were analyzed under a Nikon ECLIPSE 80i fluorescent microscope. Randomly chosen fields of at least 50 cells were quantified for EGFR and centromere 7 (CEP7)

amplification. The FISH data were analyzed by manually counting cells with EGFR or CEP7 staining. An EGFR/CEP7 ratio of >2 was considered focal amplification, whereas a ratio of <2 was considered broad amplification.

Immunoblotting Analysis

To isolate whole-cell proteins (lysates), cells were collected in an ice-cold lysis buffer (Sigma, St. Louis, MO, USA) containing protease and phosphatase inhibitors and the extracted proteins were subjected to immunoblotting, as described previously,[28] using the following primary antibodies from Cell Signaling Technology (Boston, MA, USA): phospho-EGFR (Y1068), EGFR, ERK-1/2 phospho-ERK-1/2 (Thr202/Tyr204) cleaved-PARP1, achaete-scute homolog 1 (ASCL1), and neuronal nuclei (NeuN, a mature neuron marker). β-III-tubulin and glial fibrillary acidic protein (GFAP) antibodies were purchased from Abcam (Boston, MA, USA) and Agilent (Santa Clara, CA, USA), respectively. Glyceraldehyde 3-phosphate dehydrogenase (GAPDH) antibody was purchased from Proteintech (Rosemont, IL, USA) and used as a loading control. Blots were developed using chemiluminescence-based methods and X-rays, and films were scanned (Epson, V700); Adobe Photoshop was used for linear adjustment for clarity.

RNA Isolation and Real-time Quantitative Polymerase Chain Reaction

Glioma stem-like cells (GSCs) were subjected to total RNA isolation using the RNeasy kit (Qiagen, Germantown, MD, USA) and quantified using NanoDrop. The RNA was reverse-transcribed into cDNA using a High-Capacity cDNA Reverse Transcription Kit (Applied Biosystems, Waltham, MA, USA). The gene expression levels were evaluated using an ABI-7500 Fast real-time quantitative polymerase chain reaction machine with TaqMan (Thermo Fisher Scientific, Waltham, MA, USA) master mix with specific primers for target genes, and the expression profile was calculated using the 2^{-ddct} method. GAPDH was used as an internal gene control for the relative quantification of genes. The data are presented as the relative expression of the gene of interest (fold change to control) as compared with untreated cells (control).

Flow Cytometry and Apoptosis Analyses by Annexin-V Staining

A flow cytometric analysis for evaluating apoptosis was performed by annexin-V and DAPI or PI staining. In brief, 0.5×10^6 cells were treated with trametinib (10–1 000 nM) for the indicated times. Cells were washed twice with PBS, resuspended in 100 μL of 1× annexin-V binding buffer, stained with 2–3 μL of annexin-V-FITC (BD Biosciences, Franklin Lakes, NJ, USA) antibody, and resuspended in 500 μL of annexin-V binding buffer containing 0.5–1 μg/mL DAPI or PI. The apoptotic cells were analyzed at the MD Anderson Flow Cytometry and Cellular Imaging Facility using a Gallios flow cytometer (Beckman Coulter) and analyzed using FlowJo software version 10.3.

RNA-Seq and Data Analysis

We used the pipeline for RNA sequencing data analysis pipeline[30] with the hg19 human genome assembly and the Ensembl64 transcriptome version for RNA-seq sample preprocessing to obtain reads per kilobase per million mapped reads expression values. Read counts were obtained from HT-seq[31] for the differential expression analysis using DEseq2.[32] We performed several comparisons for single and grouped GSCs (control vs post-treatment). The gene set enrichment analysis (GSEA) was performed using MSigDB[33] gene sets and 2 methods: (a) hypergeometric test selecting only the genes with absolute value fold-change ≥1 (positive for upregulated and negative for downregulated) and FDR < 0.05; and (b) running GSEA in preranked mode, ranking genes by –log10 (*P* value) and the fold-change sign.

Immunofluorescence and Immunohistochemistry

To evaluate in vitro neuronal differentiation, GSCs were plated on precoated laminin coverslips with neuronal basal media containing B27 without EGF/basic fibroblast growth factor and treated with trametinib. The cells were fixed in 4% paraformaldehyde for 15 min, rinsed with PBS at least 3 times, blocked in 5% goat serum for 1 h, and incubated with specific antibody overnight at 4°C. The slides were then washed 3 times with PBS, incubated with secondary antibody for 1 h at ambient temperature, washed 3 times, and counterstained with Vecta shield sealant containing 4′,6-diamidino-2-phenylindole (DAPI; Vector Laboratories). For immunohistochemistry and immunofluorescence staining in mouse tumors, slides were deparaffinized and subjected to gradual rehydration. Antigen retrieval was performed using citrate buffer (pH 6.0) at 95°C for 30 min, and slides were allowed to cool at ambient temperature. Slides were washed with TBS, and staining was performed as described above.

Animal Experiments and Drug Treatment

All animal studies were approved by the MD Anderson Institutional Animal Care and Use Committee (protocol #00000960-RN02). The GSCs (0.5×10^6) were implanted intracranially into the brains of nude mice (6–8 week-old females) for orthotropic xenograft using a guided bolt, as described previously.[34,35] Three days after implantation, trametinib (1 mg/kg) was administered (p.o.) by gavage for 5 consecutive days (M–F) per week. Mice were monitored daily and euthanized when they became moribund. The Kaplan-Meier method was used for survival analysis. The whole brains were collected and preserved in formaldehyde solution for histopathology and immunohistochemistry studies.

Statistical Analyses

Data were representative of at least 2 independent experiments. GraphPad Prism software was used for generating the graphs and statistical analyses.

Comparisons between 2 groups were performed by the Student *t*-test, while comparisons between more than 2 groups were analyzed by 1-way analysis of variance with corresponding Tukey's multiple comparison tests. If not indicated otherwise, analyses of significance were performed using 2-tailed tests, and $P < .05$ was considered statistically significant.

Results

EGFR Amplification is Heterogeneous in Glioblastoma and GSC Xenograft Tumors

We analyzed TCGA_glioblastoma (GBM) public data to characterize EGFR genomic alterations, including EGFR focal amplification, according to the thresholds assigned by GISTIC.[31] By using the TCGA microarray and RNA-seq EGFR data, we identified approximately 50% of glioblastoma tumors with EGFR amplification and higher mRNA expression (Figure 1A, top 2 panels). Furthermore, RNA-seq data from GSC revealed that approximately 35% of cell lines exhibited EGFR amplification, while EGFR expression was quite heterogeneous in GSC lines (Figure 1A, bottom panel).

To validate the transcriptomic findings of EGFR amplification, we used human and mouse glioblastoma tumor slides for the FISH analysis. FISH data of human glioblastoma tumors clearly showed heterogeneous amplification of EGFR, varying from no or minimal to very high amplification in a tumor-specific manner (Figure 1B and C). A similar heterogenous pattern of EGFR amplification was confirmed in mouse glioblastoma models showing varying patterns of EGFR amplification using FISH analysis (Figure 1D and E).

We further validated the above results with the protein expression of EGFR/MEK/ERK signaling molecules in 10 GSC lines using WB analysis, which showed that basal protein expression of phosphorylated EGFR (p-EGFR, Y1068), total EGFR (t-EGFR), phosphorylated ERK1/2 (p-ERK, Thr202/Tyr204), and total ERK (t-ERK) varied (heterogeneous) in the GSC cohort (Figure 1F). These results clearly established that EGFR amplification is heterogeneous in GSCs and human and mouse glioblastoma tumors.

MEK-1/2 Inhibitor Sensitivity is Primarily Associated with EGFR Amplification

We first screened 4 MEK inhibitors (GDC, MEK162, RO5, and trametinib) on a high-throughput platform in a cohort of GSC lines. An unbiased high-throughput screening showed antiproliferative activity to multiple MEK inhibitors in a set of GSC lines (sensitive, marked as green) but no activity in other lines (resistant, marked as red) (Figure 2A and Supplementary Figure S1). To validate the primary screening results, we further screened trametinib, a clinically approved MEK inhibitor, in a panel of 25 GSC lines. Approximately 50% of cell lines showed nanomolar range activity ($IC_{50} < 1$ μM), while the remainder were resistant (Figure 2B and C, and Supplementary Figure S1). Furthermore, we reported that the biological activity of trametinib was primarily associated with the focal amplification of EGFR in GSC lines (Figure 2D), which can be used

as a potential biomarker of sensitivity to MEK inhibitor (trametinib).

To determine whether constitutive MEK signaling inhibition derives the pharmacological activity of MEK inhibitors, we evaluated the expression of p-ERK1/2 in GSC11 (sensitive) and GSC8-11 (resistant) cells treated with trametinib (1–1 000 nM). To our surprise, trametinib treatment for 0.5 and 24 h significantly reduced the expression of p-ERK1/2 and t-ERK1/2 in both cell lines as compared with untreated cells (Figure 2E and F). Thus, blocking MEK/ERK signaling alone does not drive the pharmacological activity of MEK inhibitors in GSCs.

Trametinib Induced Apoptotic Cell Death in Sensitive GSCs

To investigate the mechanisms of differential activity of MEK inhibitors in GSCs, we performed cell death analysis using flow cytometry, WB analysis, and imaging. We found that trametinib treatment significantly induced dose-dependent apoptotic cell death (80% of cells undergoing apoptosis) only in sensitive GSCs (GSC11 and GSC262); no cell death was observed in resistant cells (GSC8-11) as compared with untreated cells (Figure 3A, left panels). A quantitative analysis was performed to measure trametinib-induced apoptosis in sensitive and resistant GSCs (annexin-V-positive cells; Figure 3B–D, right panel of bar graphs).

Next, we evaluated sphere formation and cell growth by microscopic study; the results indicated that trametinib treatment for 72 h significantly reduced the number and size of spheres that formed in sensitive GSCs; there was no effect on sphere formation in resistant GSCs (Figure 3E). To validate the differential effect of trametinib on apoptotic cell death, we treated 2 sensitive (GSC11 and GSC262) and 2 resistant (GSC8-11 and GSC28) cell lines with trametinib (100–1 000 nM) for 72 h and evaluated the expression of cleaved-PARP (c-PARP), an apoptotic marker, by WB analysis. Trametinib selectively induced c-PARP expression (a marker of apoptotic cell death) in sensitive cells but not in resistant cells (Figure 3F). These results indicate that trametinib selectively induced apoptotic cell death in sensitive GSCs. This differential apoptotic cell death might, in part, contribute to the pharmacological activity of the MEK inhibitor in GSCs.

RNA-Seq Identified Distinct Regulation of Neuronal Differentiation and Neurogenesis Genes in GSCs Treated with MEK Inhibitor

To understand the precise mechanism of MEK inhibitor activity, we treated 4 sensitive GSC lines (GSC11, GSC262, GSC300, and GSC23) with trametinib (50–100 nM) for 24 h and 96 h; total mRNA was subjected to RNA-seq analysis. We used the read counts obtained from RNA-seq to perform a differential expression analysis using DEseq2. Our results clearly showed that trametinib differentially regulated the expression of several hundred genes that are upregulated and downregulated in GSCs as compared with untreated cells (Figure 4A and D, and Supplementary Figure S2A and B). Furthermore,
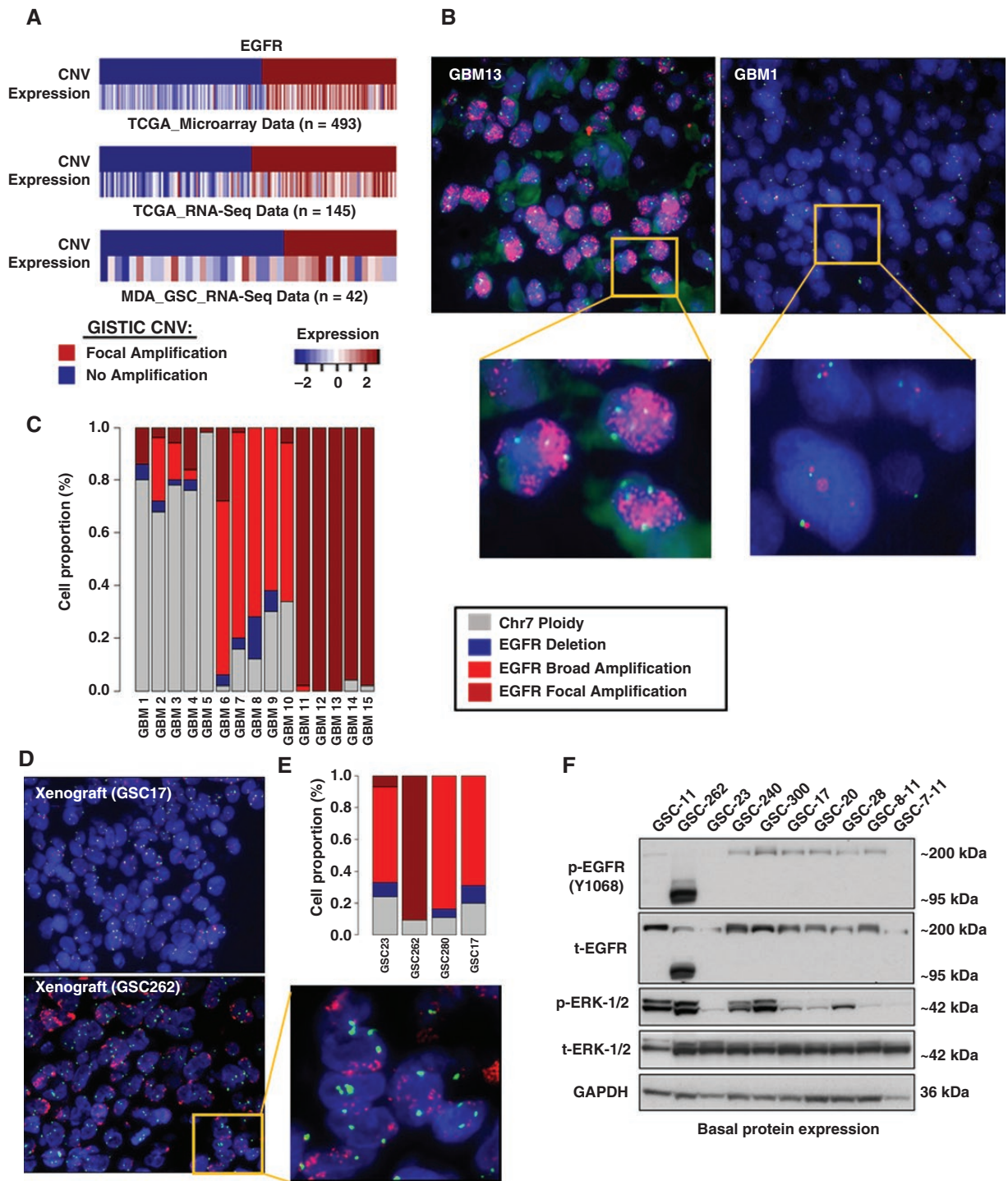
Figure 1. EGFR amplification is heterogeneous in glioblastoma. (**A**): Top 2 panels, heat map showing EGFR amplification and expression in TCGA microarray ($n = 493$) and RNA-Seq ($n = 145$) data sets of human glioblastoma. Bottom panel, heat map showing EGFR amplification and expression in RNA-Seq ($n = 42$) data sets of human GSCs. Focal EGFR amplification is defined by genome identification of significant targets in cancer and corresponding EGFR expression in TCGA and GSC data sets. (**B** and **C**): Representative images of FISH showing EGFR (green staining) and CEP7 (red staining) in human glioblastoma tumor slides. Insert showing digital magnification of the indicated region. Bar graph represents a quantitative analysis of the FISH signal for EGFR genomic alterations. For quantification of the EGFR FISH analysis, randomly chosen fields of at least 50 cells were used for EGFR and CEP7 amplification. Scale bar = 50 μm. (**D** and **E**): Representative images of FISH showing EGFR (green staining) and CEP7 (red staining) in mouse xenograft tumor slides. Insert showing digital magnification of the indicated region. Bar graph represents the quantitative analysis of FISH signal for EGFR genomic alterations. For quantification of the EGFR FISH analysis, randomly chosen fields of at least 50 cells were used for EGFR and CEP7 amplification. Scale bar = 50 μm. (**F**): Representative images of WB of p-EGFR, t-EGFR, and p-ERK-1/2 and t-ERK-1/2 in whole-cell protein lysates collected from 3D culture of a cohort of GSCs, which indicated the variable expression of EGFR/MEK/ERK signaling proteins at basal conditions.
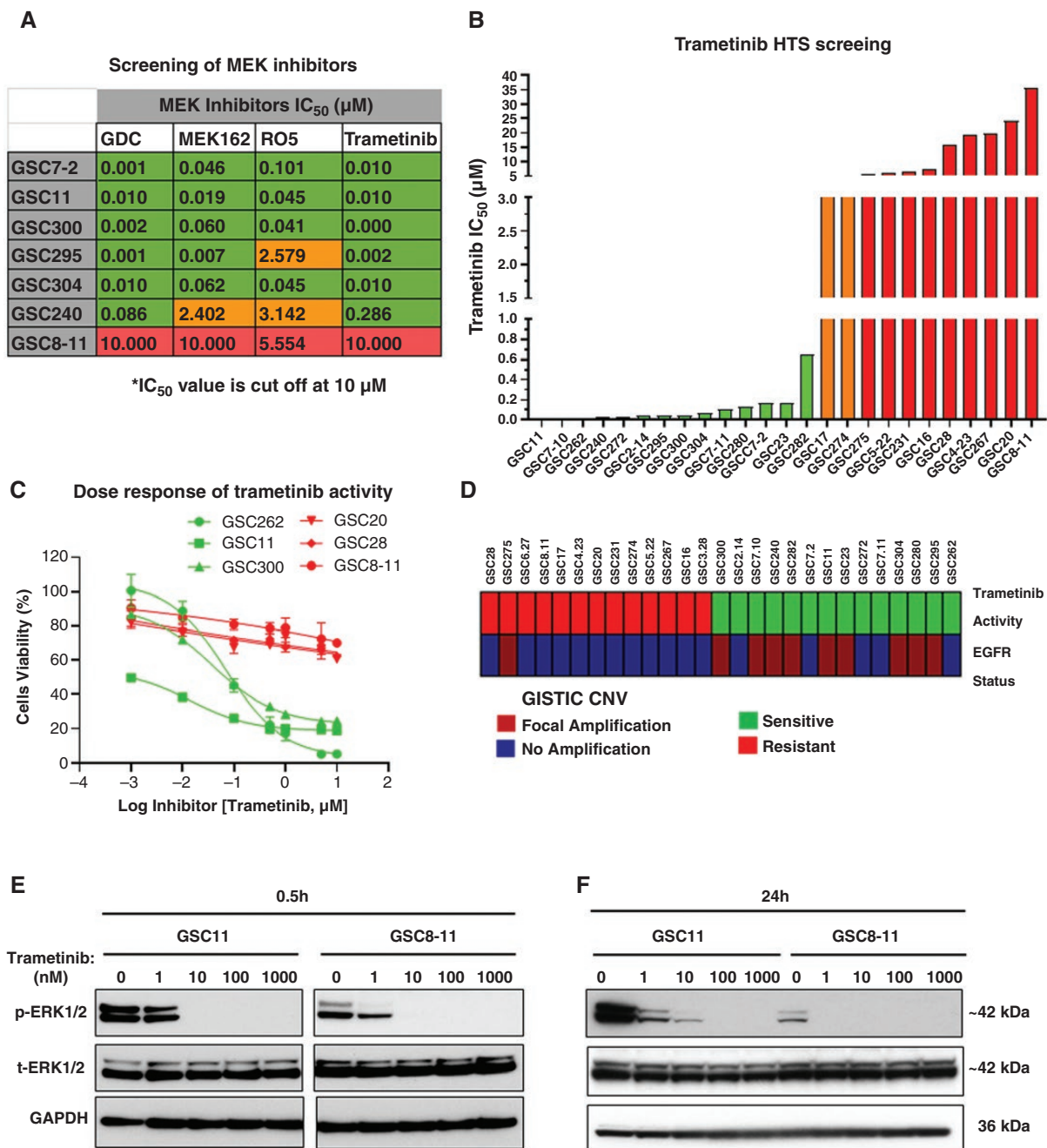
Figure 2. MEK-1/2 inhibitor sensitivity is primarily associated with EGFR amplification. (**A**) Drug screening of 4 MEK inhibitors showing the IC$_{50}$ (viability and proliferation) in 7 GSCs treated with GDC, MEK162, RO5, and trametinib (0.5–10 000 nM) for 72 h. Green indicates IC$_{50}$ < 1 (sensitive), orange indicates IC$_{50}$ > 1 < 5, and red indicates IC$_{50}$ > 5 (resistant). (**B** and **C**) Bar plot showing sensitive (green) and resistant (red) GSCs with trametinib screening in 25 GSCs; line graph shows the response of trametinib in 3 sensitive and 3 resistant cell lines. All the GSCs lines used in this study are isocitrate dehydrogenase wild-type (IDHwt) except GSC5-22. (**D**) Heat map showing the association between EGFR amplification status in GSCs and pharmacological activity of trametinib in sensitive and resistant GSCs. (**E** and **F**) Representative WB analysis of p-ERK-1/2 and t-ERK-1/2 (MEK signaling) proteins in whole-cell protein lysates of GSC11 and GSC8-11 cells treated with trametinib (1–1 000 nM) for 0.5 and 24 h, respectively.

an analysis showed increased expression of numerous neuronal differentiation marker genes in trametinib-associated upregulated signatures in GSC11 (Figure 4C) and GSC262 cells (Figure 4F), clearly indicating the induction of the neuronal differentiation signature in trametinib-treated cells.

To identify the specific biological processes and pathways that are associated with the differentially regulated genes after trametinib treatment, we performed Gene Ontology (GO) pathway analyses. The results indicated that several pathways are affected by trametinib treatment; interestingly, neuronal differentiation and neurogenesis emerged
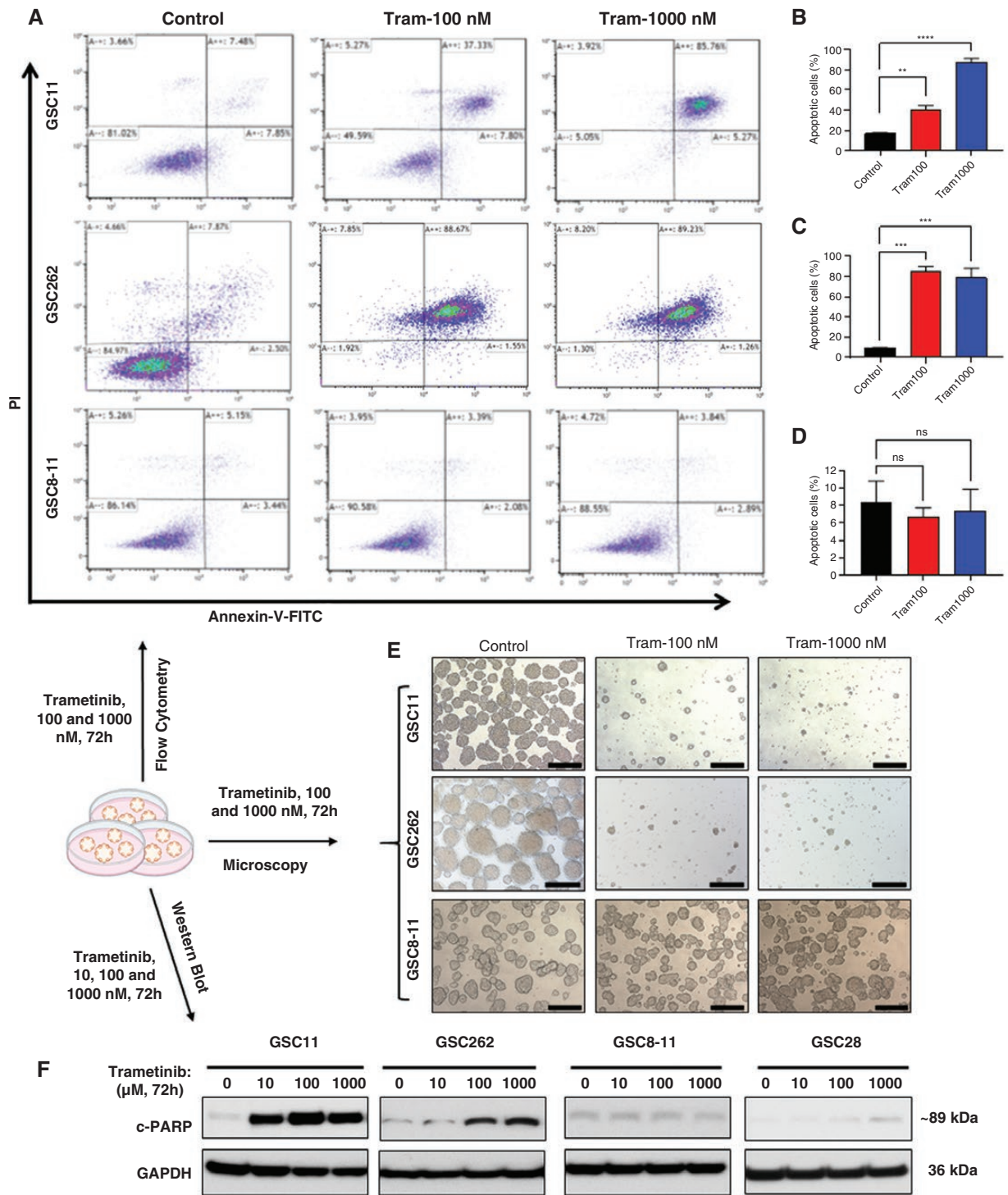
Figure 3. Trametinib treatment induced apoptotic cell death in sensitive GSCs. (A) Cells were treated with trametinib (10–1 000 nM) for 72 h, and apoptotic cell death was analyzed using flow cytometry using annexin-V-FITC and PI staining. Representative dot-plots showing dose-dependent induction of cell death in sensitive GSCs with trametinib treatment; no cell death induction was observed in the resistant GSC8-11 cell line after trametinib treatment as compared with untreated cells (control). Tram: trametinib. (B–D) Bar graphs showed quantitative analysis of trametinib-induced apoptosis in sensitive and resistant GSCs (annexin-V-positive cells). ****$P < .0001$, ***$P < .001$, and **$P < .01$ as compared with untreated cells. Tram: trametinib. (E) Representative bright field microscopy images showing the size and number of spheres of GSC11, GSC262, and GSC8-11 cells treated with trametinib (100 and 1 000 nM) for 72 h, respectively. Scale bar = 200 μm. Tram: trametinib. (F) WB analysis of apoptosis marker cleaved PARP (c-PARP) in 2 sensitive (GSC11 and GSC262) and 2 resistant (GSC8-11 and GSC28) cell lines treated with different doses of trametinib for 72 h.
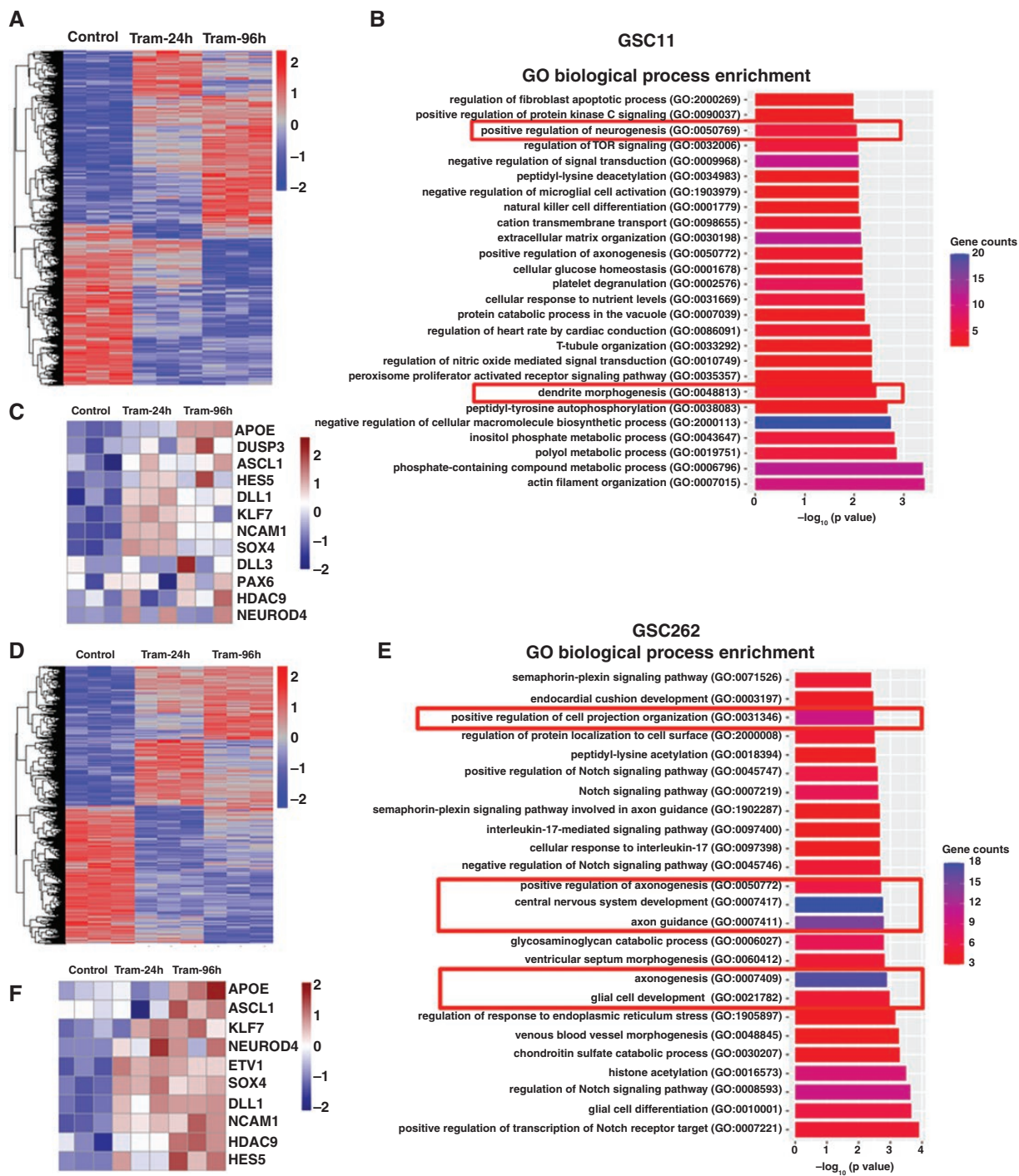
Figure 4. RNA-seq identified distinct regulation of neuronal differentiation and neurogenesis genes in GSCs treated with MEK inhibitor. (**A**, **D**) Heat maps showing the differentially expressed genes in GSC11 and GSC262 cells treated with 50 nM of trametinib for 24 h and 96 h, respectively. Read counts were obtained from HT-seq for the differential expression analysis using DEseq2. We performed several comparisons for single and grouped GSCs (control vs post-treatment). Tram: trametinib. (**C**, **F**) Heat maps showing the expression of selected neuronal genes in trametinib-treated GSC11 and GSC262 cells, respectively. Tram: trametinib. (**B**, **E**) Gene Ontology (GO) term pathway analysis with upregulated genes by trametinib treatment; red boxes indicate the pathway associated with neuronal differentiation and neurogenesis in GSC11 and GSC262 cells, respectively.

as major biological processes that are most relevant to glioblastoma biology (Figure 4B and E, and Supplementary Figure S2C). However, several other pathways are affected by trametinib treatment and are under further investigation (Figure 4B and E). Together, the comprehensive RNA-Seq analysis and GO analyses revealed that MEK inhibitor

treatment promotes the upregulation of genes involved in neuronal differentiation.

MEK Inhibition Induced Neuronal Differentiation in Sensitive GSCs

To validate the RNA-seq findings, we treated GSC11, GSC262, and GSC8-11 cells with trametinib for 72 h; the results showed increased expression of well-known neuronal differential markers, such as β-III-tubulin, ASCL1, neurogenic differentiation 4 (NeuroD4), and delta-like 3 (DLL3), in a dose-dependent manner as compared with untreated cells (Figure 5A–C and Supplementary Figure S3A and B). The neuronal differential potential of MEK inhibitors was characterized by immunofluorescence experiment by treating the sensitive and resistant GSCs with trametinib in differentiation media (neurobasal media without EGF/FGF) for 72 h and staining cells for β-III-tubulin and GFAP antibodies. The immunofluorescence results clearly showed that trametinib induced the expression of β-III-tubulin, a well-known neuronal differential marker, only in the sensitive cell line (GSC11), whereas the expression of GFAP, a well-known astrocyte marker, remained unchanged (Figure 5D).

To further validate the neuronal differential potential of MEK inhibitors, we treated GSC11, GSC262, and GSC8-11 cells with trametinib for 72 h in complete growth media and evaluated differentiation markers by WB analysis. Our findings clearly showed that MEK inhibitor increased the expression of several neuronal markers, such as β-III-tubulin, ASCL1, and NeuN (manure neuron marker), in sensitive GSCs (GSC11 and GSC262), while the expression of these markers remained unchanged in resistant GSCs (GSC8-11) (Figure 5E). Furthermore, microscopic observation confirmed neuronal differentiation induced by trametinib treatment under complete media (Supplementary Figure S3C).

We subjected differentially expressed genes from RNA-seq data of sensitive cell lines to a rank-based GSEA, which showed the enrichment of proneuronal signatures (NES = 2.13, FDR = 0.000) with trametinib-associated upregulated gene sets (Figure 5F); thus, the GSEA results indicate that GSCs are pushed towards the proneural lineage after trametinib treatment. Together, our results confirmed that MEK inhibitors (trametinib) induced neuronal differentiation in sensitive GSCs, which primarily drives antiproliferative activity in these GSC lines.

Trametinib Treatment Improved Survival and Decreased Tumor Growth and MEK/ERK Signaling in GSC Xenografts

To test the in vivo efficacy of MEK inhibitor, we orally administrated trametinib (1 mg/kg) in orthotopic xenograft (GSC11, GSC23, GSC262, and GSC8-11) glioblastoma models. Consistent with our in vitro findings, trametinib significantly prolonged the survival of GSC11 and GSC23 xenograft mouse models (EGFR-amplified or sensitive lines) as compared with vehicle control animals (Figure 6A and Supplementary Figure S4). Although trametinib treatment showed improved survival in the GSC11, GSC23,

and GSC262 xenograft models, the effect of trametinib on survival benefits in the GSC262 xenograft model is moderate which may be due to the aggressive behavior of the GSC262 cell line (Figure 6A and Supplementary Figure S4). Thus, there is not enough time for trametinib treatment to provide a more robust response. Moreover, MEK inhibition failed to improve the survival of the GSC8-11-tumor-bearing (EGFR-nonamplified or resistant line) mouse model as compared with vehicle control animals (Figure 6B). In addition, we showed a significant reduction in the cellularity and tumor size of GSC11 xenografts treated with trametinib as compared with those treated with vehicle (Figure 6C and Supplementary Figure S5). An immunohistochemistry analysis also demonstrated a significant reduction of p-ERK1/2 in mouse tumors treated with trametinib (Figure 6D).

To test the in vivo neuronal differential potential of MEK inhibition and its contribution to the antitumor activity of trametinib, we carried out immunofluorescence staining of β-III-tubulin in serial sections of GSC11 tumors; β-III-tubulin expression was analyzed within the tumor area by confocal microscopy. The immunofluorescence findings clearly showed that trametinib significantly increased the expression of β-III-tubulin (neuronal marker) within the tumor region of whole brain sections of GSC11 xenografts as compared with untreated tumors (Figure 6E and Supplementary Figure S6). Together, our data provide evidence that MEK inhibitors promote neuronal differentiation in both in vitro and in vivo models of glioblastoma, which primarily drives antitumor activity.

To corroborate the neuronal differentiation mechanism in the current study with human glioblastoma, we analyzed selected neuronal marker expression in the TCGA microarray and RNA-Seq data sets using the GlioVis platform.[23] The results of our analysis indicated that the expression of neuronal marker genes, such as β-III-tubulin, is decreased in tumor tissue as compared with nontumor tissue (Figure 6F and G). Additional neuronal markers, such as neural cell adhesion molecule 1 (NCAM1), microtubule-associated protein 2 (MAP2), synaptophysin, and neurofilament, heavy polypeptide (NEFH), are also significantly downregulated in glioblastoma tumors as compared with nontumor tissue (Supplementary Figure S7). Further analysis using the TCGA_GBMLLG data set showed that the expressions of neuronal signatures genes are low in the high-grade (grade IV) glioma tumors as compared with the low-grade (grade II and III) tumors with the EGFR amplification (gain of chromosome7 and loss of chrpmosome10) (Supplementary Figure S8A–C). To evaluate the impact of EGFR amplification on the survival and expression of neuronal genes under altered EGFR (amplification) status, we analyzed the TCGA glioblastoma RNA-seq data with EGFR-amplified tumors and EGFR nonamplified tumors using cBioPortal (TCGA, Firehose Legacy). Our analysis showed that patients with EGFR-amplified tumors have poor survival outcomes as compared with patients with EGFR nonamplified tumors (Supplementary Figure S8D). However, the expressions of neuronal signature genes (NeuroD4, ASCL1, SYP, MAP2, and NEFH) are relatively unchanged in the EGFR amplified and EGFR nonamplified tumors (Supplementary Figure S8E–I).
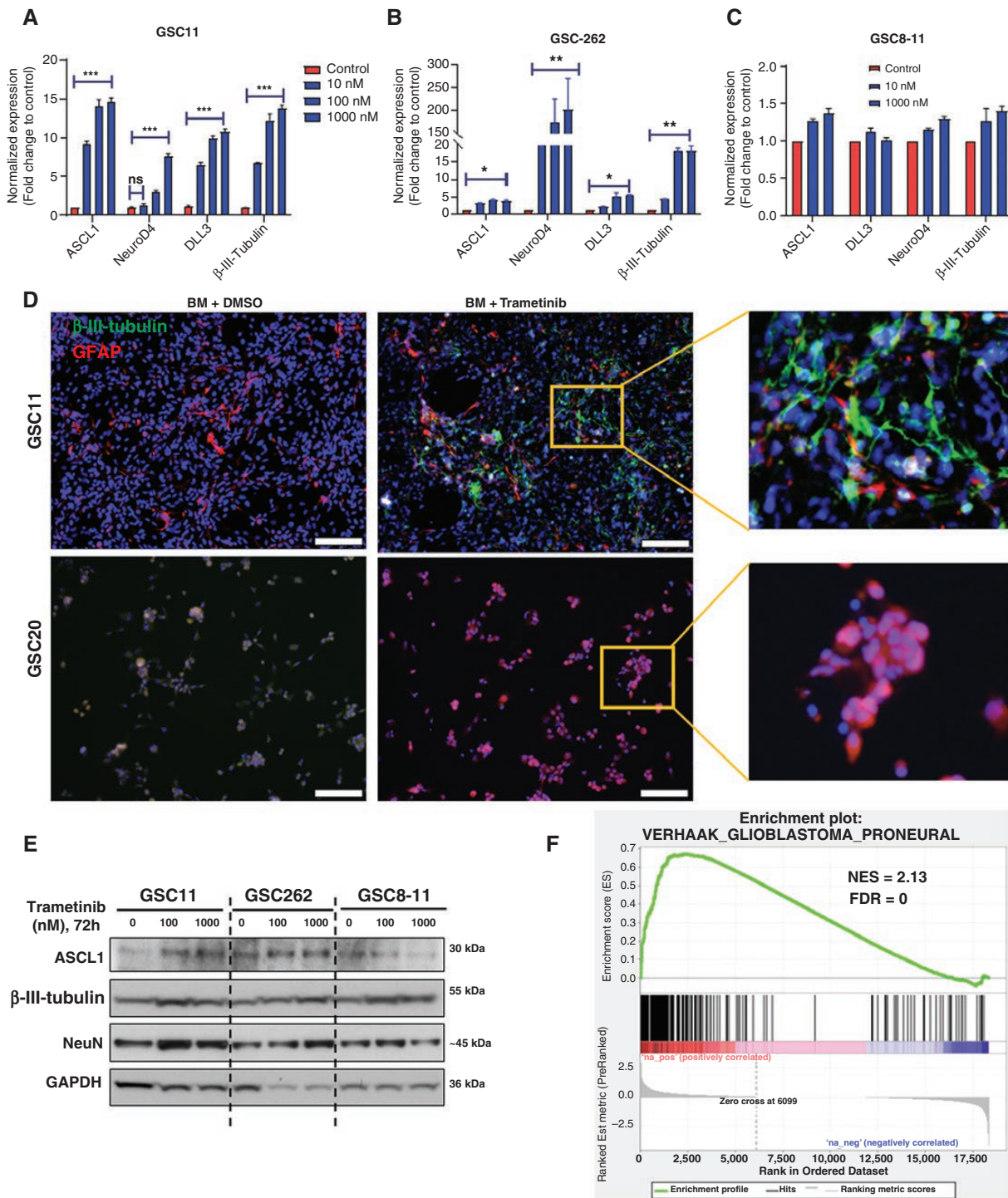
Figure 5. MEK inhibition induced neuronal differentiation in sensitive GSCs. (**A–C**) mRNA expression of neuronal differentiation genes, ASCL1, NeuroD4, DLL3, and β-III-tubulin in GSCs treated with trametinib (10–1 000 nM) for 72 h. ***P < .001, **P < .01, and *P < .05 as compared with untreated cells. (**D**) Representative images showing neuronal differentiation of GSCs in BM media (neurobasal media without EGF and FGF) treated with trametinib for 72 h and stained for β-III-tubulin (green, neuronal marker) and GFAP (red, astrocyte marker). Insert showing digital magnification of the indicated region. Scale bar = 100 μm. (**E**) WB analysis of the neuronal differentiation markers β-III-tubulin, ASCL1, and NeuN in 2 sensitive (GSC11 and GSC262) and 1 resistant (GSC8-11) cell line treated with different doses of trametinib for 72 h. (**F**) GSEA of differentially expressed genes with trametinib treatment for the association of the proneural phenotype of glioblastoma (as defined by Verhaak et al.[5]). The x-axis represents genes, ordered by expression changes between treated and untreated. The cumulative enrichment score is represented on the y-axis.
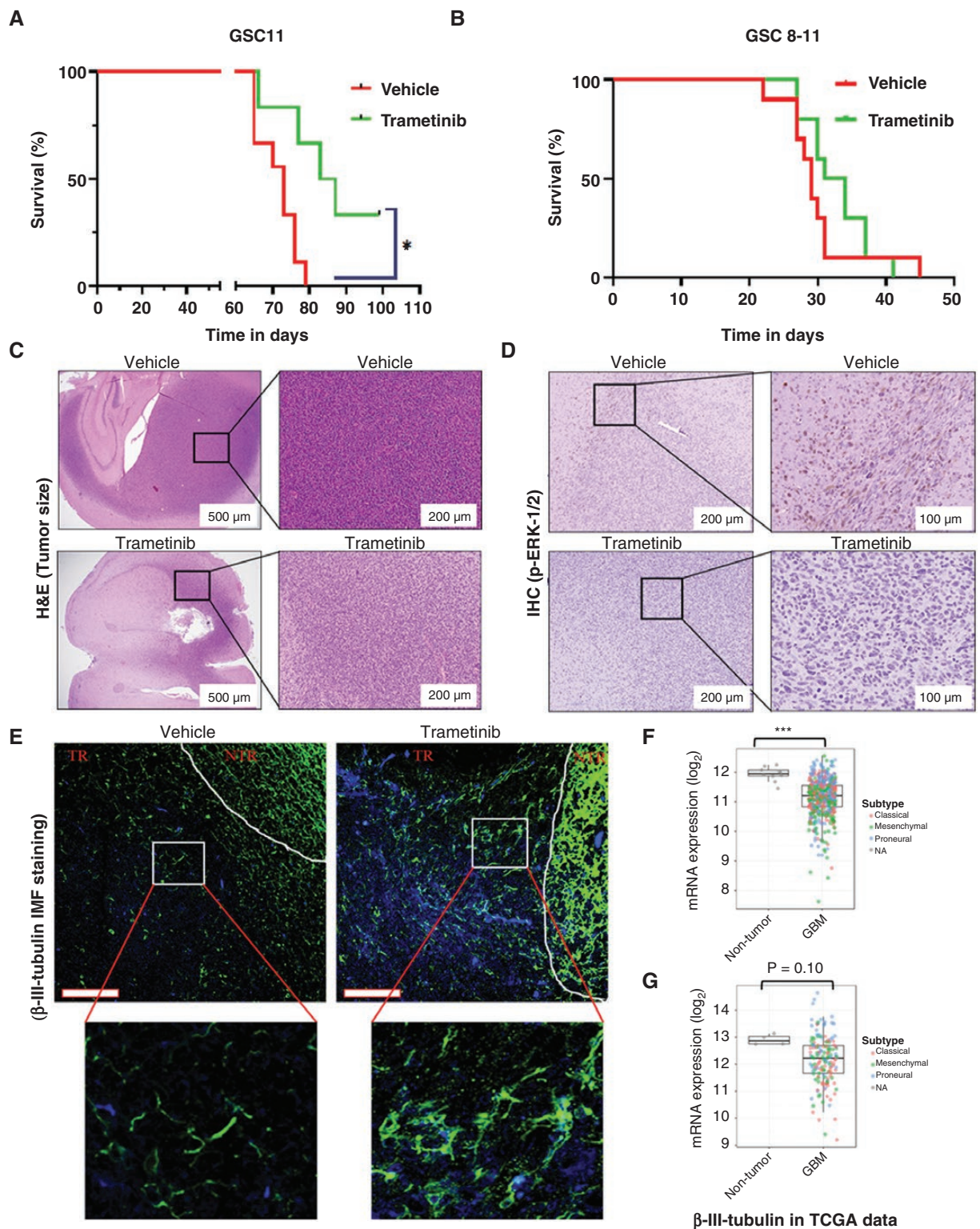
Figure 6.   Trametinib treatment improved survival and decreased cell proliferation and MEK/ERK signaling in GSC xenografts. (**A** and **B**) Kaplan-Meier survival curve showing the survival of animals intracranially implanted with GSC11 (sensitive) and GSC8-11 (resistant) cell lines and treated with trametinib (1 mg/kg) 5 consecutive days (M-F) per week (n = 8–10). (**C** and **D**) Representative images of histopathology (H&E) and immunohistochemistry showing tumor size and cellularity of GSC11 xenografts, as well as expression of p-ERK-1/2 in vehicle- and trametinib-treated mouse tumors, respectively (n = 5–6). Insert showing digital magnification of indicated regions. Scale bar, 500 μm, 200 μm, and 100 μm, respectively. (**E**) Representative immunofluorescence images of β-III-tubulin (neuronal marker) in GSC11 xenografts of vehicle control and trametinib-treated mouse tumor sections (n = 5). Insert showing digital magnification of indicated regions. TR = tumor region, and NTR = nontumor region. Scale bar = 100 μm. (**F** and **G**) Bar graphs show β-III-tubulin expression in TCGA microarray (10 nontumors and 528 glioblastomas) and RNA-Seq (4 nontumors, and 156 glioblastomas) data sets analyzed using the GlioVis platform. ***P < .001.

Finally, we evaluated the association between neuronal differential gene expression and survival outcomes in glioma and glioblastoma patients in the TCGA, Chinese Glioma Genome Atlas, and Rembrandt data sets using the GlioVis platform. We found that high expression of neuronal differential genes, such as NeuroD4, MAP2, NEFH, and synaptophysin, was associated with prolonged overall survival in glioma and glioblastoma patients (Supplementary Figure S9). Thus, this analysis confirmed that antitumor activity via neuronal differentiation mechanisms is not limited to our in vitro and in vivo experiments but also plays an important role in controlling human glioblastoma and prolonging survival outcomes.

Discussion

The GSCs exhibit the heterogeneous nature of glioblastoma tumors and greatly contribute to therapy resistance and disease recurrence. It is noteworthy that the majority of data analyzed in this study was described as per the previous WHO classification (WHO 2016)[36] for CNS tumors. Therefore, the implication of our findings in therapeutic applications needs careful examination, especially in the context of IDH-1 mutant glioma tumors.[8,37] Here, our findings demonstrated that both glioblastoma and GSCs possess constitutive heterogeneous amplification of EGFR and activated MEK1/2-ERK1/2 signaling. Screening of multiple MEK inhibitors showed antiproliferative and apoptotic cell death in GSCs with activated EGFR/MEK/ERK signaling. A mechanistic investigation revealed that MEK inhibitors promoted neurogenesis and neuronal differentiation (upregulation of β-III-tubulin, ASCL1, DLL3, and NeuroD4) in a series of in vitro and in vivo experiments. Finally, we reported the antitumor efficacy of an orally active MEK inhibitor, trametinib, in an orthotopic glioblastoma (2 out of 3 sensitive line) model, accompanied by the promotion of neuronal differentiation. Thus, the induction of neuronal differentiation might contribute to the antiproliferative and antitumor activity of MEK inhibitors and could be efficacious in the treatment of glioblastoma patients with activated EGFR/MEK/ERK signaling.

The MEK1/2/ERK-1/2 pathway has been implicated in several cellular aspects of glioblastoma, such as the maintenance of stemness, cell proliferation, differentiation, migration, and invasion.[15,16] Several MEK1/2 inhibitors have been tested clinically or are currently undergoing clinical evaluation for the treatment of multiple cancers.[17] MEK inhibitor screening in our study clearly showed antiproliferative effects in approximately 50% of GSC lines, while the remaining lines were resistant to multiple MEK inhibitors, irrespective of the inhibition of MEK/ERK signaling. Moreover, the evaluation of the cell death potential of MEK inhibitors showed a differential response to MEK inhibitor pharmacological activity because only sensitive GSCs (GSC11 and GSC262) undergo apoptotic cell death in a dose-dependent manner, while resistant cells did not show any apoptotic cell death. Our results are in agreement with those of a recent clinical trial of trametinib in combination with dabrafenib, which showed good efficacy in patients with BRAF V600E mutation–positive recurrent

or refractory high- and low-grade glioma.[19] Another MEK inhibitor, selumetinib, is also approved for the treatment of neurofibromatosis type I tumors in children. Thus, the present findings provide further evidence of the pharmacological efficacy of MEK inhibitors in glioblastoma.

Glioma stem-like cells (GSCs) play a critical role in glioblastoma tumor initiation and therapy resistance because of their capacity to self-renew and differentiate into all major central nervous system cell types, leading to tumor heterogeneity.[38,39] Although the role of RAS and downstream MEK1/2-ERK1/2 activation in stem cells and cancer has been an area of intense research for decades, it remains unclear how the activation of these pathways promotes an undifferentiated state, which in glioma is associated with tumorigenicity and therapy resistance.[40] There has been tremendous interest in developing differentiation therapies that target GSCs because there are few effective therapeutic strategies for glioblastoma.[41] The RNA-seq results in our study revealed that trametinib treatment significantly promoted neuronal differentiation, as evidenced by the increased expression of ASCL1, NeuroD4, and DLL3, in a dose-dependent manner, in sensitive GSCs. This novel biological effect of MEK inhibitors was also characterized in an immunofluorescence experiment under differentiation conditions (neurobasal media without EGF/FGF) in which trametinib induced the expression of β-III-tubulin (Figure 5). The neuronal differentiation potential of MEK inhibitor was attributed to the increased expression of β-III-tubulin, ASCL1, and NeuN, only in sensitive GSCs (GSC11 and GSC262); however, the expression of these neuronal markers did not change in resistant cells. These findings are in agreement with those of Sabelström et al.'s study, which highlighted that neuronal differentiation abrogates the aggressive phenotype of glioblastoma via reversal of the ERK1/2-miR-124-SOX9 axis.[42] Another study showed that MEK inhibitors promote neuronal differentiation in rat and mouse neural stem cells by reversing the suppressive roles of MEK2 in neurogenesis.[43,44]

Treatments that target cancer stem cell differentiation have been proposed as promising therapies for many cancer types.[45] For example, retinoic acid or NOTCH signaling inhibitors, have been shown to induce GSC differentiation.[46] Park and co-workers have reported that a sustained expression of ASCL1 or NOTCH inhibition induces neuronal differentiation and reduces the tumourigenic capacity of GSCs and suggested the regulatory role of ASCL1 in GSCs deferrization.[47] Another study has shown that bone morphogenic protein 4 (BMP4) triggers the suppressor of mothers against decapentaplegic signaling in GSCs independent of the EGFR level.[48] They reported that GSCs with different EGFR levels (low vs high) responded differently to temozolomide (TMZ) treatments, and BMP4-mediated differentiation in GSC with high-EGFR-induced apoptosis and enhanced the TMZ response, in contrast, GSCs with low-EGFR did not underwent apoptosis and did not affect the TMZ response. This study supports our findings that MEK inhibition induced neuronal differentiation and apoptotic cell death in EGFR-amplified GSCs. In addition, Lee et al. have reported that glioblastoma stem cells (U87) can reprogram and differentiate into neurons using a cocktail of small molecule inhibitors.[49]

Furthermore, the results of a human glioblastoma data analysis using the GlioVis platform indicated lower expression of neuronal marker genes, such as MAP2, synaptophysin, NEFH, Stathmin 1, and NCAM1 in glioblastoma tumors than in nontumor tissue, whereas high expression of NeuroD4, MAP2, NEFH, and synaptophysin is associated with the prolonged overall survival of patients. The results of these analyses corroborated with the antitumor activity in our mouse glioblastoma experiment highlighting a potential contribution of neuronal differentiation as an additional pharmacological effect of MEK inhibitors. Thus, the present study also provides a new direction for exploring neuronal differentiation mechanisms to identify new treatment strategies for glioblastoma.

In summary, our results showed that MEK inhibitors (trametinib) promote neuronal differentiation, which might contribute to the antiproliferative and antitumor activity. Our study identified the neuronal differentiation activity of MEK inhibition in glioblastoma, as a potential additional mechanism of action of MEK1/2 inhibitors. Thus, MEK1/2 inhibitors could be an effective treatment for glioblastoma patients with active EGFR/MAPK signaling tumors. However, the precise mechanism and key regulators that mediate this neuronal differentiation process need further investigation.

Supplementary material

Supplementary material is available online at *Neuro-Oncology* (https://academic.oup.com/neuro-oncology).

Keywords

apoptosis | EGFR-MEK signaling | glioblastoma | MEK inhibitors | neuronal differentiation

Conflicts of interest statement

J.F.D. is consulting/advisory board member for Carthera, Haihe Pharmaceuticals, MundiPharma, Insightec, BioAsis Technologies, Kintara, Kazia, Monteris Medical, Karyopharm, Sumitomo Dainippon Pharma Oncology, Merck, Sapience, VBI Vaccines, Chimerix, Midatech, Aucentra Therapeutics, Servier, Telix, Alpha Pharmaceuticals, Chimerix, and Cure Brain Cancer Foundation. W.K.A.Y. serves as a consultant with DNATrix, Roche, and Denovo. The rest of the authors have no conflicts of interest to disclose.

Authorship statement

Designed the study: S.K., J.F.D., V.B., and W.K.A.Y.; conducted the experiment and analyzed the data: S.K., J.D., and V.B.; bioinformatic analysis: R.M. and E.M.; wrote the main draft: S.K.; and review and editing: S.K., D.K., W.K.A.Y., J.F.D., V.B., S.Y.P., and Y.P. All authors read and approved the final manuscript.

Data availability

All data generated or analyzed during this study are included in this article. TCGA publicly available data sets were analyzed in this study, which can be found here: FireBrowse site of the Broad Institute.

References

1. Preusser M, de Ribaupierre S, Wohrer A, et al. Current concepts and management of glioblastoma. *Ann Neurol*. 2011;70(1):9–21.
2. Alvarado AG, Thiagarajan PS, Mulkearns-Hubert EE, et al. Glioblastoma cancer stem cells evade innate immune suppression of self-renewal through reduced TLR4 expression. *Cell Stem Cell*. 2017;20(4):450–461.e4.
3. Patel AP, Tirosh I, Trombetta JJ, et al. Single-cell RNA-seq highlights intratumoral heterogeneity in primary glioblastoma. *Science*. 2014;344(6190):1396–1401.
4. Safa AR, Saadatzadeh MR, Cohen-Gadol AA, Pollok KE, Bijangi-Vishehsaraei K. Glioblastoma stem cells (GSCs) epigenetic plasticity and interconversion between differentiated non-GSCs and GSCs. *Genes Dis*. 2015;2(2):152–163.
5. Verhaak RG, Hoadley KA, Purdom E, et al.; Cancer Genome Atlas Research Network. Integrated genomic analysis identifies clinically relevant subtypes of glioblastoma characterized by abnormalities in PDGFRA, IDH1, EGFR, and NF1. *Cancer Cell*. 2010;17(1):98–110.
6. Stichel D, Ebrahimi A, Reuss D, et al. Distribution of EGFR amplification, combined chromosome 7 gain and chromosome 10 loss, and TERT promoter

mutation in brain tumors and their potential for the reclassification of IDHwt astrocytoma to glioblastoma. *Acta Neuropathol.* 2018;136(5):793–803.

7. Felsberg J, Hentschel B, Kaulich K, et al.; German Glioma Network. Epidermal growth factor receptor variant III (EGFRvIII) positivity in EGFR-amplified glioblastomas: prognostic role and comparison between primary and recurrent tumors. *Clin Cancer Res.* 2017;23(22):6846–6855.

8. Whitfield BT, Huse JT. Classification of adult-type diffuse gliomas: Impact of the World Health Organization 2021 update. *Brain Pathol.* 2022;32(4):e13062.

9. Georgescu MM. Multi-platform classification of IDH-Wild-Type Glioblastoma based on ERK/MAPK pathway: Diagnostic, prognostic and therapeutic implications. *Cancers (Basel).* 2021;13(18):4532.

10. Eskilsson E, Røsland GV, Solecki G, et al. EGFR heterogeneity and implications for therapeutic intervention in glioblastoma. *Neuro Oncol.* 2018;20(6):743–752.

11. Gao SP, Mark KG, Leslie K, et al. Mutations in the EGFR kinase domain mediate STAT3 activation via IL-6 production in human lung adenocarcinomas. *J Clin Invest.* 2007;117(12):3846–3856.

12. Oprita A, Baloi SC, Staicu GA, et al. Updated insights on EGFR signaling pathways in Glioma. *Int J Mol Sci.* 2021;22(2):587.

13. Thorne AH, Zanca C, Furnari F. Epidermal growth factor receptor targeting and challenges in glioblastoma. *Neuro Oncol.* 2016;18(7):914–918.

14. Reardon DA, Wen PY, Mellinghoff IK. Targeted molecular therapies against epidermal growth factor receptor: Past experiences and challenges. *Neuro Oncol.* 2014;16(Suppl 8):viii7–vii13.

15. Selvasaravanan KD, Wiederspohn N, Hadzalic A, et al. The limitations of targeting MEK signalling in Glioblastoma therapy. *Sci Rep.* 2020;10(1):7401.

16. Racke FK, Lewandowska K, Goueli S, Goldfarb AN. Sustained activation of the extracellular signal-regulated kinase/mitogen-activated protein kinase pathway is required for megakaryocytic differentiation of K562 cells. *J Biol Chem.* 1997;272(37):23366–23370.

17. Frémin C, Meloche S. From basic research to clinical development of MEK1/2 inhibitors for cancer therapy. *J Hematol Oncol.* 2010;3(1):8.

18. Menzies AM, Yeh I, Botton T, et al. Clinical activity of the MEK inhibitor trametinib in metastatic melanoma containing BRAF kinase fusion. *Pigment Cell Melanoma Res.* 2015;28(5):607–610.

19. Wen PY, Stein A, van den Bent M, et al. Dabrafenib plus trametinib in patients with BRAF(V600E)-mutant low-grade and high-grade glioma (ROAR): A multicentre, open-label, single-arm, phase 2, basket trial. *Lancet Oncol.* 2022;23(1):53–64.

20. Gross AM, Wolters PL, Dombi E, et al. Selumetinib in Children with Inoperable Plexiform Neurofibromas. *N Engl J Med.* 2020;382(15):1430–1442.

21. Harvard. BIoM. The Broad Institute TCGA GDAC Firehose Browse portal. 2019; 2017. http://firebrowse.org/.

22. Mermel CH, Schumacher SE, Hill B, et al. GISTIC20 facilitates sensitive and confident localization of the targets of focal somatic copy-number alteration in human cancers. *Genome Biol.* 2011;12(4):R41.

23. Bowman RL, Wang Q, Carro A, Verhaak RG, Squatrito M. GlioVis data portal for visualization and analysis of brain tumor expression datasets. *Neuro Oncol.* 2017;19(1):139–141.

24. Weinstein JN, Collisson EA, Mills GB, et al.; Cancer Genome Atlas Research Network. The Cancer Genome Atlas Pan-Cancer analysis project. *Nat Genet.* 2013;45(10):1113–1120.

25. Zhao Z, Meng F, Wang W, et al. Comprehensive RNA-seq transcriptomic profiling in the malignant progression of gliomas. *Sci Data.* 2017;4:170024.

26. Madhavan S, Zenklusen JC, Kotliarov Y, et al. Helping personalized medicine become a reality through integrative translational research. *Mol Cancer Res.* 2009;7(2):157–167.

27. Jiang H, Gomez-Manzano C, Aoki H, et al. Examination of the therapeutic potential of Delta-24-RGD in brain tumor stem cells: role of autophagic cell death. *J Natl Cancer Inst.* 2007;99(18):1410–1414.

28. Khan S, Mahalingam R, Sen S, et al. Intrinsic interferon signaling regulates the cell death and mesenchymal phenotype of glioblastoma stem cells. *Cancers.* 2021;13(21):5284.

29. Wu S, Gao F, Zheng S, et al. EGFR amplification induces increased DNA damage response and renders selective sensitivity to Talazoparib (PARP Inhibitor) in Glioblastoma. *Clin Cancer Res.* 2020;26(6):1395–1407.

30. Torres-García W, Zheng S, Sivachenko A, et al. PRADA: Pipeline for RNA sequencing data analysis. *Bioinformatics.* 2014;30(15):2224–2226.

31. Anders S, Pyl PT, Huber W. HTSeq--a Python framework to work with high-throughput sequencing data. *Bioinformatics.* 2015;31(2):166–169.

32. Love MI, Huber W, Anders S. Moderated estimation of fold change and dispersion for RNA-seq data with DESeq2. *Genome Biol.* 2014;15(12):550.

33. Subramanian A, Tamayo P, Mootha VK, et al. Gene set enrichment analysis: A knowledge-based approach for interpreting genome-wide expression profiles. *Proc Natl Acad Sci.* 2005;102(43):15545–15550.

34. Lal S, Lacroix M, Tofilon P, et al. An implantable guide-screw system for brain tumor studies in small animals. *J Neurosurg.* 2000;92(2):326–333.

35. Ding J, Li X, Khan S, et al. EGFR suppresses p53 function by promoting p53 binding to DNA-PKcs: A noncanonical regulatory axis between EGFR and wild-type p53 in glioblastoma. *Neuro Oncol.* 2022;24(10):1712–1725.

36. Louis DN, Perry A, Reifenberger G, et al. The 2016 World Health Organization classification of tumors of the central nervous system: A summary. *Acta Neuropathol.* 2016;131(6):803–820.

37. Louis DN, Wesseling P, Aldape K, et al. cIMPACT-NOW update 6: New entity and diagnostic principle recommendations of the cIMPACT-Utrecht meeting on future CNS tumor classification and grading. *Brain Pathol.* 2020;30(4):844–856.

38. Nobusawa S, Lachuer J, Wierinckx A, et al. Intratumoral patterns of genomic imbalance in glioblastomas. *Brain Pathol.* 2010;20(5):936–944.

39. Alcantara Llaguno SR, Parada LF. Cell of origin of glioma: biological and clinical implications. *Br J Cancer.* 2016;115(12):1445–1450.

40. An Z, Aksoy O, Zheng T, Fan QW, Weiss WA. Epidermal growth factor receptor and EGFRvIII in glioblastoma: Signaling pathways and targeted therapies. *Oncogene.* 2018;37(12):1561–1575.

41. Dirks PB. Brain tumor stem cells: the cancer stem cell hypothesis writ large. *Mol Oncol.* 2010;4(5):420–430.

42. Sabelström H, Petri R, Shchors K, et al. Driving neuronal differentiation through reversal of an ERK1/2-miR-124-SOX9 axis abrogates glioblastoma aggressiveness. *Cell Rep.* 2019;28(8):2064–2079.e11.

43. Lee HR, Lee J, Kim HJ. Differential effects of MEK inhibitors on rat neural stem cell differentiation: Repressive roles of MEK2 in neurogenesis and induction of astrocytogenesis by PD98059. *Pharmacol Res.* 2019;149:104466.

44. Li M, Tsang KS, Choi ST, et al. Neuronal differentiation of C172 neural stem cells induced by a natural flavonoid, baicalin. *ChemBioChem.* 2011;12(3):449–456.

45. de Thé H. Differentiation therapy revisited. *Nat Rev Cancer.* 2018;18(2):117–127.

46. De Silva MI, Stringer BW, Bardy C. Neuronal and tumourigenic boundaries of glioblastoma plasticity. *Trends Cancer.* 2023;9(3):223–236.

47. Park NI, Guilhamon P, Desai K, et al. ASCL1 reorganizes chromatin to direct neuronal fate and suppress Tumorigenicity of glioblastoma stem cells. *Cell Stem Cell.* 2017;21(2):209–224.e7.

48. Ciechomska IA, Gielniewski B, Wojtas B, Kaminska B, Mieczkowski J. EGFR/FOXO3a/BIM signaling pathway determines chemosensitivity of BMP4-differentiated glioma stem cells to temozolomide. *Exp Mol Med.* 2020;52(8):1326–1340.

49. Lee C, Robinson M, Willerth SM. Direct reprogramming of glioblastoma cells into neurons using small molecules. *ACS Chem Neurosci.* 2018;9(12):3175–3185.